Raman study of ion-induced defects in *N*-layer graphene

2010 J. Phys.: Condens. Matter 22 334204

(http://iopscience.iop.org/0953-8984/22/33/334204)

J. Phys.: Condens. Matter **22** (2010) 334204 (5pp) doi:10.1088/0953-8984/22/33/334204

Raman study of ion-induced defects in *N*-layer graphene

Ado Jorio[1,2], Marcia M Lucchese[2], Fernando Stavale[2], Erlon H Martins Ferreira[2], Marcus V O Moutinho[3], Rodrigo B Capaz[2,3] and Carlos A Achete[2,4]

[1] Departamento de Física, Universidade Federal de Minas Gerais, Belo Horizonte, MG, 30123-970, Brazil
[2] Divisão de Metrologia de Materiais, Instituto Nacional de Metrologia, Normalização e Qualidade Industrial (INMETRO), Duque de Caxias, RJ, 25250-020, Brazil
[3] Instituto de Física, Universidade Federal do Rio de Janeiro, Caixa Postal 68528, Rio de Janeiro 21941-972, RJ, Brazil
[4] Programa de Engenharia Metalúrgica e de Materiais (PEMM), Universidade Federal do Rio de Janeiro, Caixa Postal 68505, Rio de Janeiro 21945-970, RJ, Brazil

E-mail: adojorio@fisica.ufmg.br

Received 31 December 2009, in final form 5 February 2010
Published 4 August 2010
Online at stacks.iop.org/JPhysCM/22/334204

Abstract
Raman scattering is used to study the effect of low energy (90 eV) Ar^+ ion bombardment in graphene samples as a function of the number of layers N. The evolution of the intensity ratio between the G band (1585 cm^{-1}) and the disorder-induced D band (1345 cm^{-1}) with ion fluence is determined for mono-, bi-, tri- and ∼50-layer graphene samples, providing a spectroscopy-based method to study the penetration of these low energy Ar^+ ions in AB Bernal stacked graphite, and how they affect the graphene sheets. The results clearly depend on the number of layers. We also analyze the evolution of the overall integrated Raman intensity and the integrated intensity for disorder-induced versus Raman-allowed peaks.

1. Introduction

Disorder-induced symmetry-breaking plays a very important role in the determination of several material properties, such as transport properties and the relaxation of photo-excited carriers [1]. Raman spectroscopy has become a key technique and is widely used to characterize and identify disorder in the sp^2 network of different carbon structures, such as graphite intercalated compounds [2–4], nanostructured carbon [5], carbon nanofibers and nanotubes [6], as well as fullerenes [7]. The presence of disorder in sp^2 hybridized carbon systems leads to rich and intriguing phenomena in their resonance Raman spectra, thus making Raman spectroscopy one of the most sensitive and informative techniques to characterize disorder in sp^2 carbon materials.

In the Raman scattering process, a photon generates an electron–hole pair (green arrows in figure 1(a)) and the excited electron is further scattered by phonons, as indicated by the black arrows. Due to momentum conservation requirements in periodic systems, the first-order Raman scattering process generates only Γ-point phonons (wavevector $q = 0$). Such a process is pictured in figure 1(a) by the downward black arrow labeled G (from graphite), indicating electron–phonon energy exchange with no wavevector variation. As shown in figure 1(b), the Raman spectrum of pristine graphene exhibits this G mode, which is related to the in-plane stretching of the C–C bonds [6]. When the periodic lattice of graphene is broken by defects, the momentum conservation requirement is broken and all the phonons in the Brillouin zone become Raman-allowed, which could result in a phonon-density-of-states-like Raman spectrum. However, resonant electron–phonon scattering processes connecting real electronic states (indicated by the solid black arrows connecting red bullets in figure 1(a)) are predominant [8, 9] and energy conservation requirements impose that the Raman spectrum of disordered graphene (see figure 1(c)) exhibits only two new sharp features at 1345 cm^{-1} (D band) and 1626 cm^{-1} (D′ band). These intervalley (D) and intravalley (D′) defect-induced double-resonance scattering processes occur within an area close to a defect that has been named the 'activated area' and this area is determined by the Raman scattering coherence length [10]. These processes are also the ones mainly responsible for electron decoherence in

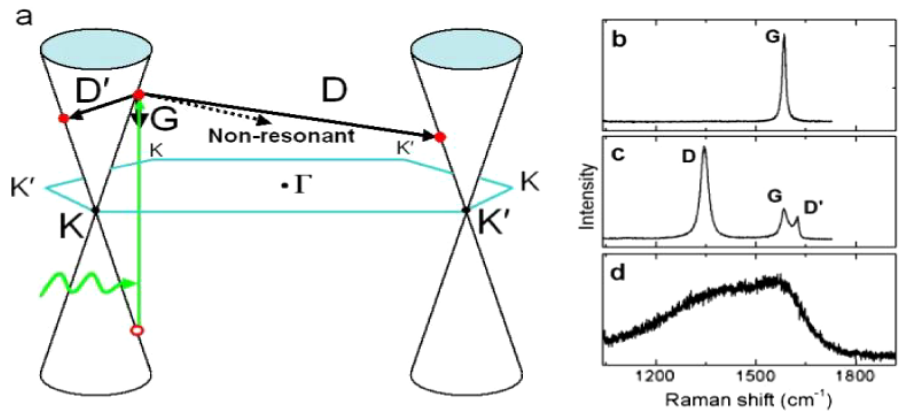

Figure 1. (a) Schematics showing the electronic dispersion near the Fermi level at the K and K′ points in the hexagonal Brillouin zone of graphene. The light-induced electron–hole formation and the different categories of electron–phonon scattering processes are indicated by green and black arrows, respectively. The graphics on the right show the first-order Raman spectra of crystalline (b), defective ((c), 10^{13} Ar^+ cm^{-2}) and fully disordered ((d), 10^{15} Ar^+ cm^{-2}) single-layer graphene deposited on an SiO_2 substrate (see the text for more details). The D, G and D′ peaks are labeled.

(This figure is in colour only in the electronic version)

optics and transport phenomena in sp^2 carbon atoms [11–13]. Finally, when the periodic system is fully disordered by large ion fluences (above 10^{13} Ar^+ cm^{-2}), this 'activated area' gives way to an effectively 'disordered area', where the hexagonal lattice has been effectively destroyed and the electron and phonon momenta are no longer good quantum numbers. As shown in figure 1(d), the Raman spectrum of fully disordered single-layer graphene resembles the profile of the density of states (DOS) for the higher energy optical phonon branch [6].

Recently we have used Raman scattering to study the evolution of disorder in monolayer graphene (1-LG) subjected to low energy (90 eV) Ar^+ ion bombardment. These low energy ions have been experimentally confirmed to barely exceed the threshold value for the displacement of surface C atoms (∼47 eV in HOPG), thereby avoiding cascade effects [14, 15]. The evolution of the intensity ratio I_D/I_G between the G band (1585 cm^{-1}) and the disorder-induced D band (1345 cm^{-1}) with ion fluence was determined, providing a spectroscopy-based method to accurately quantify the density of defects in 1-LG. A phenomenological model was proposed to describe the non-monotonic evolution of I_D/I_G with the density of defects (or with the average distance between defects), based on a competition between the 'activated area' and the 'disordered area' with increasing defect concentration. From this model, the Raman scattering coherence length l = 2 nm was obtained [10]. Here we extend such a study to graphene as a function of the number of layers N.

2. Experimental details

Several graphene samples with different numbers of layers were prepared from a single mechanical exfoliation of highly oriented pyrolytic graphite (HOPG-ZYB grade, 20 mm × 20 mm × 2 mm, NT-MDT Company) and deposited onto an Si substrate with a 300 nm thick layer of SiO_2, following a nowadays widely used procedure [16]. No further cleaning or processing was applied to the graphene samples to avoid changing its pristine properties. Optical microscopy was used to map the graphene sample location on the Si/SiO_2 substrate [16]. The number of layers for each graphene sample was identified by both Raman spectroscopy [17] and atomic force microscopy (AFM instrument from JPK Company, in the tapping mode under ambient conditions). We located four samples to study and discuss here: (i) 1-LG, (ii) bi-layer (2-LG), (iii) tri-layer (3-LG) and (iv) a small HOPG flake, ∼50 layers in thickness, as inferred from its AFM height. The graphene samples were all about 2–3 μm × 3–4 μm, which guarantees the laser focus (∼1 μm^2) was always fully reaching the graphene samples.

Ion bombardment experiments (with a partial argon pressure lower than 2×10^{-5} mbar) were carried out in an OMICRON VT-STM ultra-high vacuum system (base pressure 5.0×10^{-11} mbar) equipped with an ISE 5 ion source. The ion beam incidence angle was 45° with respect to the normal direction of the sample's surface. Low energy ions (90 eV) were used to produce the structural defects. Five ion fluences were used, namely 10^{11}, 10^{12}, 10^{13}, 10^{14} and 10^{15} Ar^+ cm^{-2}. The ion fluence was calibrated by direct counting of defects, using scanning tunneling spectroscopy, as described in [10]. The distance between defects and the sizes of the 'activated' and 'disordered' areas are in the 1–50 nm range [10], which means the results are homogeneous within the laser focus (∼1 μm^2).

Micro-Raman scattering measurements were performed with a Horiba Jobin Yvon T6400 triple-monochromator equipped with a N_2-cooled charge-coupled device (CCD) detector. We employed the backscattering configuration, using a 100× objective (∼1 μm^2 beam spot on the sample). The excitation laser energy was 2.41 eV (514.5 nm). A low power (0.25 mW at the microscope objective) was used to avoid heat-induced sample damage or graphitization. The Si/SiO_2 substrate Raman peak in the 950–1000 cm^{-1} range was measured and used to check the Raman intensity calibration.

3. Results and discussions

Figure 2(a) shows the evolution of the Raman disorder parameter I_D/I_G as a function of ion bombardment fluence for 1-LG, 2-LG, 3-LG and ∼50-LG (HOPG). The different stages observed for the non-monotonic evolution of disorder in 1-LG graphene [10] are shown in figure 2 by the large increase, saturation and decrease of the I_D/I_G ratio. These stages are better distinguished for the monolayer graphene and evolve into the smoother HOPG response [18] as the number of layers increases. The maximum I_D/I_G for most of the samples is achieved for the 10^{13} Ar^+ cm^{-2} fluence, and their values at this ion fluence are 3.30:1.58:1.17:0.18 for 1-LG:2-LG:3-LG:50-LG, respectively. Therefore, the maximum I_D/I_G values observed in 2-LG and 3-LG graphene are, respectively, ∼1/2 and ∼1/3 of the values in 1-LG, i.e. I_D/I_G scales with the number of layers N. This result is directly related to the contribution from untouched layers, i.e. it provides evidence that the low energy ion impact induces defects limited to one layer (not necessarily the first). Due to its low energy, a simple ion does not create defects in many layers. The process is most probably limited to one defect per Ar^+ ion. Compagnini *et al* [19] performed similar experiments with C+ ions, but using a much larger energy (500 keV). The maximum I_D/I_G values they observed in 2:3-LG was 7:5 = 1.4. While the absolute values should not be compared because they used a different excitation laser line, the ratio was far from 2, meaning in their case one high energy ion can cause more than one defect. A bulk HOPG sample has also been measured and the evolution is very similar to the results shown for the ∼50-layer graphene, although the I_D/I_G is 3.5 times smaller for bulk HOPG. This is in agreement with a penetration depth of about 150 layers.

In figure 2(b) we multiplied the I_D/I_G ratio by the number of layers N for each sample. Assuming each low energy Ar^+ ion is producing only one defect in one graphene layer, this N-normalized I_D/I_G ratio is equivalent to normalizing the evolution of disorder, irrespective of the number of carbon atoms in the sample. Figure 2(b) shows that, for low ion fluences (below 10^{13} Ar^+ cm^{-2}), the evolution of disorder is similar for the four samples, independent of N. For larger ion fluences (above 10^{13} Ar^+ cm^{-2}), amorphization takes place and the I_D/I_G ratio decreases when the number of layers is small. Notice that 10^{15} Ar^+ cm^{-2} corresponds to one ion per C atom for a 1-LG. The value of $N(I_D/I_G)$ for the final 10^{15} Ar^+ cm^{-2} ion fluence also scales with N.

Figure 2(c) shows the evolution of the integrated area in the frequency range where the D and G peaks are observed (1200–1700 cm^{-1}). While the absolute values are meaningless because they depend on experimental conditions, the evolution of the integrated area by varying just the number of defects provides interesting insights. Except for the two last points for 1-LG and 2-LG, where the number of ions/C atom reaches full disorder, there is a monotonic increase in the D + G integrated area with increasing disorder. This shows that the effect of increasing disorder actually opens more channels for the inelastic scattering process, thus increasing the overall area for the Raman spectra. The overall dependence is basically independent of N for 1-LG, 2-LG and 3-LG except, of course,

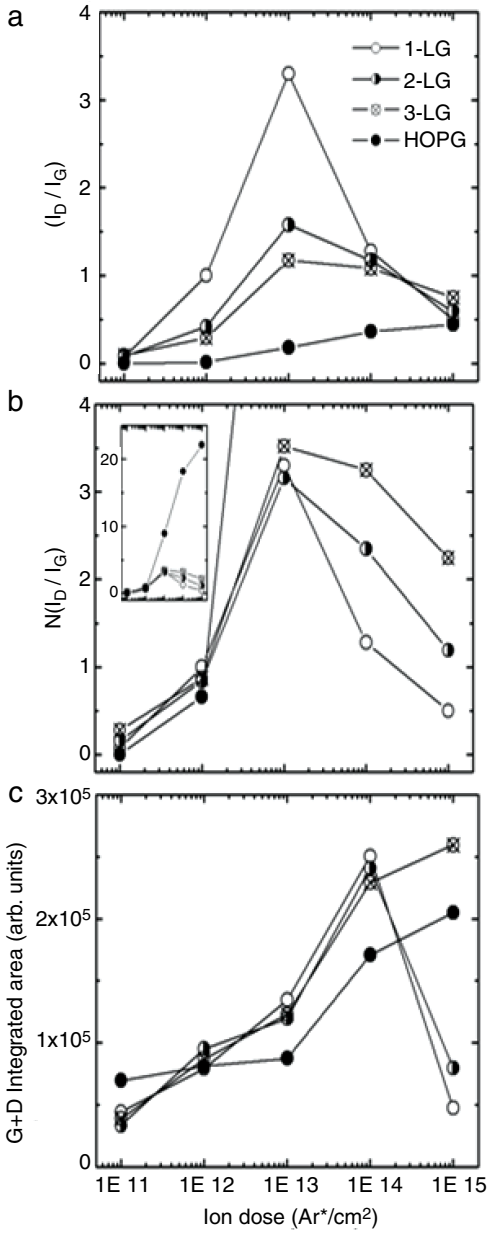

Figure 2. (a) Evolution of disorder in graphene as a function of the number of layers. The D versus G Raman band intensity ratios (I_D/I_G) are plotted as a function of ion bombardment fluence for (○) 1-LG, (◑) 2-LG, (⊗) 3-LG and (●) ∼50-LG (HOPG). (b) The same plot as in (a), but the (I_D/I_G) values have been multiplied by the number of layers N. The inset shows the details of the large increase in (I_D/I_G) for the ∼50-LG sample. (c) The evolution of the D + G integrated area as a function of the ion fluence. The values displayed here were all obtained using a Lorentzian fitting of the spectra.

for the fully disordered systems subjected to the highest ion fluence. The dependence is distinct for the ∼50-LG. This result can be related to the penetration depth. The evolution of the electric field when the sample becomes thicker has to be taken into account to fully rationalize this difference.

Although the overall Raman scattering increases with increasing disorder, as shown in figure 2(c), this increase has to be related to defect-induced processes. To analyze this argument, in figure 3 we plot the integrated area of the

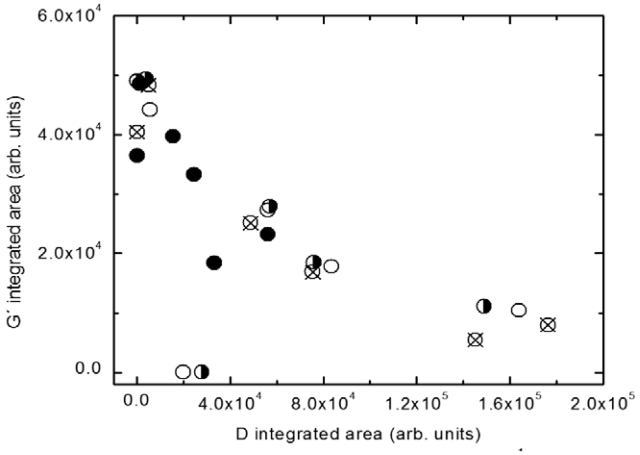

Figure 3. Integrated area under the G′ Raman peak (∼2700 cm^{-1}) as a function of the integrated area under the D band Raman peak (∼1350 cm^{-1}). The values come from Lorentzian fitting of the peaks. The number of peaks within the G′ and D bands varies with the number of layers, as previously determined [17]. For the highest ion fluence (10^{15} Ar^{+} cm^{-2}) there is an overlap between the D and G peaks, and the fitting is not unique. However, the fitting uncertainty is not large enough to change the trends shown in this figure.

Raman-allowed G′ band as a function of the integrated area for the disorder-induced D band. The G′ band is a two-phonon Raman feature, roughly an overtone of the D band (G ∼ 2D). While the D band area increases, the G′ band area decreases. Therefore, figure 3 shows there is a competition between the Raman-allowed and the disorder-induced inelastic scattering processes. Data from the four samples analyzed in this work are plotted in figure 3 showing, again, a common behavior that is independent of the number of layers N. Here even the ∼50-LG follows the same trend, since the differences related to the penetration depth are rationalized out by comparing the results from two Raman features on the same sample. The decrease in the G′ band integrated area is due to the opening of channels for one-phonon D band processes, thus decreasing the probability for the two-phonon (G′ ∼ 2D) processes. The increase in the D band integrated area is much stronger than the decrease in the G′ integrated area, and this is due to the large increase in the D bandwidth. The smaller the distance between the defects, the larger the uncertainty for the phonon wavevectors fulfilling the double-resonance disorder-induced Raman processes [8, 9]. This increase evolves until reaching the phonon DOS-like profile shown in figure 1(d). At this point, the G′ intensity is basically absent for the few-layer graphene samples. For HOPG, the number of untouched layers is always capable of providing intense G and G′ bands.

4. Summary

In this paper we study the evolution of the disorder effects in the Raman spectra from graphene as a function of the number of graphene layers N. The I_D/I_G behavior was observed to scale with N, clearly demonstrating the lower energy ions we used here were not able to cause cascade effects, but the process is limited generally to one defect per bombarding ion. For few-layer graphene samples ($N = 1, 2, 3$), the normalized evolution of I_D/I_G increases on increasing the number of defects (increasing the 'activated area' [10]), and further saturates and decreases. This decrease is due to the take-over of the 'activated area' by the 'disordered area', as introduced previously for 1-LG [10]. However, the decrease in I_D/I_G for larger ion fluences is less evident the larger the N. For many-layer graphene (∼50 and higher), the normalized evolution of I_D/I_G on increasing the number of defects is a monotonic increase, since there are always more graphene layers to be bombarded.

Our results also show that the disorder increases the overall Raman integrated area, i.e. more channels are opened for the inelastic scattering of light. There is competition between Raman-allowed and disorder-induced peaks, but in general the overall integrated area increases. This increase seems to be independent of the number of layers.

Acknowledgments

The authors acknowledge financial support from CNPq, FINEP, FAPERJ and AFOSR/SOARD (award no. FA9550-08-1-0236).

References

[1] Castro-Neto A H, Guinea F, Perer N M and Geim A K 2009 The electronic properties of graphene *Rev. Mod. Phys.* **81** 109
[2] Eklund P C, Dresselhaus G, Dresselhaus M S and Fischer J E 1977 Raman scattering from in-plane lattice modes in low stage graphite-alkali metal compounds *Phys. Rev.* B **16** 3330
[3] Eklund P C, Dresselhaus G, Dresselhaus M S and Fischer J E 1980 Raman scattering in graphite–lithium intercalation compounds *Phys. Rev.* B **21** 4705
[4] Eklund P C, Smith D S, Murthy V R K and Leung S Y 1980 Optical studies of the high-frequency graphitic intralayer phonons in graphite-$SbCl_5$ *Synth. Metals* **2** 99
[5] Ferrari A C and Robertson J 2000 Interpretation of Raman spectra of disordered and amorphous carbon *Phys. Rev.* B **61** 14095
[6] Dresselhaus M S and Eklund P C 2000 Phonons in carbon nanotubes *Adv. Phys.* **49** 705
[7] Dresselhaus M S, Dresselhaus G and Eklund P C 1996 *Science of Fullerenes and Carbon Nanotubes* (New York, NY: Academic)
[8] Thomsen C and Reich S 2000 Double resonant Raman scattering in graphite *Phys. Rev. Lett.* **85** 5214
[9] Saito R, Jorio A, Souza Filho A G, Dresselhaus G, Dresselhaus M S and Pimenta M A 2002 Probing phonon dispersion relations of graphite by double resonance Raman scattering *Phys. Rev. Lett.* **88** 027401
[10] Lucchese M M, Stavale F, Martins Ferreira E H, Vilani C, Moutinho M V M, Capaz R B, Achete C A and Jorio A 2010 Quantifying ion-induced defects and Raman relaxation length in graphene *Carbon* **48** 1592–7
[11] Perebeinos V, Tersoff J and Avouris Ph 2005 Effect of exciton-phonon coupling in the calculated optical absorption of carbon nanotubes *Phys. Rev. Lett.* **94** 027402
[12] Bonini N, Lazzeri M, Marzari N and Mauri F 2007 Phonon anharmonicities in graphite and graphene *Phys. Rev. Lett.* **99** 176802
[13] Rutter G M, Crain J N, Guisinger N P, Li T, First P N and Stroscio J A 2008 Scattering and interference in epitaxial graphene *Science* **317** 219

[14] Hahn J R and Kang H 1999 Vacancy and interstitial defects at graphite surfaces: scanning tunneling microscopy study of the structure, electronic property, and yield for ion induced defect creation *Phys. Rev.* B **60** 6007
[15] Marton D, Bu H, Boyd K J, Todorov S S, Al-Bayati A H and Rabalais J W 2005 On the defect structure due to low energy ion bombardment of graphite *Surf. Sci. Lett.* **326** L489
[16] Geim A K and Novoselov K S 2007 The rise of graphene *Nat. Mater.* **6** 183
[17] Ferrari A C *et al* 2006 Raman spectrum of graphene and graphene layers *Phys. Rev. Lett.* **97** 187401
[18] Jorio A, Lucchese M M, Stavale F and Achete C A 2009 Raman spectroscopy study of Ar^+ bombardment in highly oriented pyrolytic graphite *Phys. Status Solidi* b **246** 2689
[19] Compagni G, Giannazzo F, Sonde S, Raineri V and Ramini E 2009 Ion irradiation and defect formation in single layer graphene *Carbon* **47** 3201